ARTICLE IN PRESS

Transportation Research Part C xxx (2017) xxx–xxx

Contents lists available at ScienceDirect

Transportation Research Part C

journal homepage: www.elsevier.com/locate/trc

Data-driven spatio-temporal discretization for pedestrian flow characterization

Marija Nikolić *, Michel Bierlaire

Transport and Mobility Laboratory, School of Architecture, Civil and Environmental Engineering, École Polytechnique Fédérale de Lausanne, Station 18, CH-1015 Lausanne, Switzerland

ARTICLE INFO

Article history:
Received 15 August 2017
Received in revised form 29 August 2017
Accepted 30 August 2017
Available online xxxx

Keywords:
Pedestrian flow
Time and space discretization
Three-dimensional Voronoi diagrams
Individual trajectories
Robust indicators

ABSTRACT

We propose a novel approach to pedestrian flow characterization. The definitions of density, flow and velocity existing in the literature are extended through a data-driven spatio-temporal discretization framework. The framework is based on three-dimensional Voronoi diagrams. Synthetic data is used to empirically investigate the performance of the approach and to illustrate its advantages. Our approach outperforms the considered approaches from the literature in terms of the robustness with respect to the simulation noise and with respect to the sampling frequency. Additionally, the proposed approach is by design (i) independent from an arbitrarily chosen discretization; (ii) appropriate for the multidirectional composition of pedestrian traffic; (iii) able to reflect the heterogeneity of the pedestrian population; and (iv) applicable to pedestrian trajectories described either analytically or as a sample of points.

1. Introduction

Research on pedestrian traffic has received growing attention during the last decades due to its importance in many aspects: planning of walking facilities under regular and safety-critical circumstances, operations in large events, description of congestion, etc. All these aspects require a sophisticated understanding and modeling of the data behind complex pedestrian movement patterns (Bierlaire and Robin, 2009). Data collection for pedestrian flow and behavior analysis used to be particularly cumbersome. Typically, manual counting methods (on-site or on videos) and surveys distributed to randomly selected individuals were the main sources of data. Nowadays, automatic pedestrian detection and tracking methods have evolved tremendously, allowing for more comprehensive analyses (Bauer et al., 2009; Alahi et al., 2014a,b; Seer et al., 2014).

To increase insights into pedestrian movements, different empirical studies were conducted and reported in the literature (Lam et al., 1995; Hoogendoorn and Daamen, 2004; Helbing et al., 2005; Schadschneider et al., 2009). For instance, it was observed that directness, habits, pleasantness, safety, pollution and noise levels are some of the important attributes for pedestrian route choice (Bovy and Stern, 2012). Other empirical studies have revealed the existence of relationships between traffic indicators (Weidmann, 1993). Self-organized structures in pedestrian flows, such as lane formation (Daamen and Hoogendoorn, 2003; Hoogendoorn and Daamen, 2004), and phenomena like stop and go waves (Helbing et al., 2007), herding (Helbing et al., 2005), the faster is slower (Helbing and Johansson, 2010), the zipper effect (Hoogendoorn and Daamen, 2005), were also empirically discovered.

* Corresponding author.
E-mail addresses: marija.nikolic@epfl.ch (M. Nikolić), michel.bierlaire@epfl.ch (M. Bierlaire).

http://dx.doi.org/10.1016/j.trc.2017.08.026
0968-090X/

Please cite this article in press as: Nikolić, M., Bierlaire, M. Data-driven spatio-temporal discretization for pedestrian flow characterization. Transport. Res. Part C (2017), http://dx.doi.org/10.1016/j.trc.2017.08.026

The empirical observations have inspired a number of theories and models of pedestrian movements. They are utilized to describe and predict pedestrian movement at strategic, tactical, and operational level (Hoogendoorn and Bovy, 2004). The models concerned with strategic decisions (departure time choice, activity pattern choice) are important for the assessment of pedestrian demand (Danalet et al., 2014). The models at tactical level are focused on activity scheduling and route-choice (Cheung and Lam, 1998; Stubenschrott et al., 2014). Together with the models at operational level (walking behavior), they are used to evaluate quality levels of pedestrian traffic, and have been applied to support the design and planning processes in many areas related to pedestrians (Daamen, 2004). The modeling of pedestrian walking behavior attracts a significant attention. For instance, there are approaches that are based on social force-fields (Helbing and Molnar, 1995; Zeng et al., 2014), cellular automata (Blue and Adler, 2001; Hsu and Chu, 2014), continuum flow (Hughes, 2002; Hoogendoorn et al., 2014, 2015), utility maximization (Robin et al., 2009) and queuing theory (Cheah and Smith, 1994; Løvås, 1994). A comprehensive review of the existing approaches and their evaluation can be found in Duives et al. (2013).

The fundamental variables used at both levels, to observe and to model the traffic of pedestrians, are density (k), flow (q) and velocity (v). *Density* is expressed as the number of pedestrians per unit of space at a given moment in time; *flow* is interpreted as the number of pedestrians per unit of time and per unit of length; *velocity* is expressed in meters per unit of time. Several definitions of these variables are proposed in the literature (Duives et al., 2015; Zhang, 2012). However, little concern is dedicated to the nature of spatial and temporal discretization underlying the definitions. The basic issue is that there are many possible ways to discretize continuous space and time for the purpose of defining traffic variables. Yet, studies normally report the analysis for one particular discretization scheme whose choice is often arbitrary.

Although advanced theories and pedestrian models at strategic, tactical, and operational level exit, the fundamental aspects related to pedestrian movement are still not adequately treated. The aim of this study is to utilize the potential of the data obtained using state-of-the-art tracking technologies to address this point. This becomes essential in the context of the growing data revolution and interconnected technologies that can help improve the safety and convenience of pedestrians. We propose a discretization framework that is independent from arbitrarily chosen values, and that results in a realistic and robust pedestrian flow characterization. Our approach is data-driven, and it is based on spatio-temporal Voronoi diagrams designed through the utilization of pedestrian trajectory data.

The structure of the paper is as follows. A review of related research from the literature is provided in Section 2. Section 3 provides a formal introduction of the basic elements involved in our analysis. Section 4 describes the proposed methodology for the derivation of the spatio-temporal discretization framework. Based on this framework, we derive the definitions of the pedestrian traffic variables, that is density, flow and velocity. Section 5 empirically illustrates the performance of the approach by using synthetic data. Finally, Section 6 summarizes the outcomes of the proposed methodology and determines future research directions.

2. Literature review

The issue of discretization is well recognized in geography (Openshaw, 1984; Çöltekin et al., 2011) and dynamic systems (Beck and Roepstorff, 1987). The research from the field of geography have demonstrated that the results of any spatio-temporal analysis depend severely on the underlying discretization. The problem appears in two dimensions, space and time (known as Modifiable Areal Unit Problem and Modifiable Temporal Unit Problem). For instance, analysis of data using grid-based spatial discretization differs from analysis performed using hexagon cells. Similarly, temporal discretization may distort or exaggerate the actual temporal pattern existing in data if it is based on an arbitrary choice. It is therefore essential that the discretization rely on a meaningful basis relevant for the purpose of the study. The definition of discretization scheme has to precede any attempt to define characteristics based on it.

This section first focuses on vehicular traffic characterization, that is relevant for pedestrian as well. However, for most applications in pedestrian flow theory the definitions derived in the field of vehicular traffic can not be directly used. In comparison to roadways where vehicular flow is regulated and separated by directions, the lack of strict rules for pedestrians to follow allows them to occupy any part of the walkable area and to move in a multi-directional fashion. We then present the approaches specific to pedestrian traffic characterization and their comparison.

2.1. Vehicular traffic

The most general and widely used definitions of vehicular traffic variables are proposed by Edie (1963). The definitions are derived based on the trajectories of vehicles $i = 1, \ldots, N$ in the time-space region A. The shape of the region A is usually rectangular with duration dt and length dx. The definitions are given as

$$k(A) = \frac{\sum_{i=1}^{N} t_i}{dxdt}, \tag{1}$$

$$q(A) = \frac{\sum_{i=1}^{N} x_i}{dxdt}, \tag{2}$$

Please cite this article in press as: Nikolić, M., Bierlaire, M. Data-driven spatio-temporal discretization for pedestrian flow characterization. Transport. Res. Part C (2017), http://dx.doi.org/10.1016/j.trc.2017.08.026

$$v(A) = \frac{\sum_{i=1}^{N} x_i}{\sum_{i=1}^{N} t_i}, \tag{3}$$

where t_i and x_i are the time spent by vehicle i, respectively the distance traversed by vehicle i in the region A. This approach is applicable to any time-space domain of interest and provides consistent results in observations and modeling. The determination of the shape, the size and the placement of the time-space region A is however left to the modeler.

Some authors propose a "vehicle-based" discretization (Jabari et al., 2014; Treiber and Kesting, 2013). The definitions of the indicators with this discretization are consistent with the classical definitions of Edie (1963), but with the space-time intervals chosen to fit exactly one vehicle each. Let $x_{i-1}(t)$ and $x_i(t)$ denote the positions of the leader, $i-1$, and the follower, i, at time t. The spacing is defined as $s_i(t) = x_{i-1}(t) - x_i(t)$. The density at time t is defined as the inverse of the spacing $s_i(t)$ measured at that time

$$k(x,t) = \frac{1}{s_i(t)}, \quad \text{for} \quad x \in [x_i(t), x_{i-1}(t)). \tag{4}$$

Let $t_i(x)$ denote the time when vehicle i crosses position x. The time headway is defined as $h_i(x) = t_i(x) - t_{i-1}(x)$. The flow at position x is defined as the inverse of the time headway $h_i(x)$ measured at that location

$$q(x,t) = \frac{1}{h_i(x)}, \quad \text{for} \quad t \in (t_{i-1}(x), t_i(x)]. \tag{5}$$

Speed is defined as the ratio between flow and density

$$v(x,t) = \frac{s_i(t)}{h_i(x)}, \quad \text{for} \quad x \in [x_i(t), x_{i-1}(t)), t \in (t_{i-1}(x), t_i(x)], \tag{6}$$

and it represents a mean speed for vehicle i. This approach is microscopic, and thus, it allows to preserve the heterogeneity of driver population (Jabari et al., 2014).

2.2. Pedestrian traffic

In this section we first present a general description of the approaches available in the field of pedestrian traffic. Then, the theoretical and technical differences of the approaches are discussed.

2.2.1. Description of methods

One of the first approaches to pedestrian flow characterization was proposed by Fruin (1971). In this method a grid-based spatial discretization is considered and density is defined as

$$k(x,y,t) = \frac{N_A(t)}{|A|}, \quad \text{for} \quad (x,y) \in A, \tag{7}$$

where A is a grid cell, $|A|$ is the area of A, and $N_A(t)$ represents the number of pedestrians present in the cell A at a specific time instant t. The instantaneous velocity of pedestrian i at t is specified using the following formulation

$$\vec{\boldsymbol{v}}_i(t) = \frac{\begin{pmatrix} x_i(t_2) \\ y_i(t_2) \end{pmatrix} - \begin{pmatrix} x_i(t_1) \\ y_i(t_1) \end{pmatrix}}{t_2 - t_1}, \tag{8}$$

where $(x_i(t), y_i(t))^T$ refers to the position of pedestrian i, and t_1 and t_2 define the time instants before, respectively after time t. In general, no guidance is provided for the selection of these time instants. The velocity within the cell A is then given as the average of individual instantaneous velocities

$$\vec{\boldsymbol{v}}(x,y,t) = \frac{\sum_{i=1}^{N_A} \vec{\boldsymbol{v}}_i(t)}{N_A}, \quad \text{for} \quad (x,y) \in A. \tag{9}$$

The flow is determined using the fundamental flow equation

$$\vec{\boldsymbol{q}}(x,y,t) = k(x,y,t)\, \vec{\boldsymbol{v}}(x,y,t). \tag{10}$$

In the rest of the paper, we refer to this method as the grid-based method (GB), as in Duives et al. (2015).

The range-based method (RB) is similar to the grid-based method (Duives et al., 2015). The difference is that a circle defined by radius r at any discrete location in space is used instead of rectangular cells.

In van Wageningen-Kessels et al. (2014), similar to Saberi et al. (2014), the definitions of Edie (1963) are extended by studying pedestrian traffic in a three-dimensional time–space diagram A (of length dx, width dy and duration dt) with pedestrians $i = 1, \ldots, N$. The density is defined as the average number of pedestrians in the region $[dx \times dy]$ during time period dt

$$k(A) = \frac{\sum_{i=1}^{N} t_i}{dxdydt}, \tag{11}$$

Please cite this article in press as: Nikolić, M., Bierlaire, M. Data-driven spatio-temporal discretization for pedestrian flow characterization. Transport. Res. Part C (2017), http://dx.doi.org/10.1016/j.trc.2017.08.026

where t_i is the time during which pedestrian i is present in the region A. The flow is defined in x and y directions as

$$\vec{\boldsymbol{q}}(A) = \begin{pmatrix} q_x(A) \\ q_y(A) \end{pmatrix} = \begin{pmatrix} \frac{\sum_{i=1}^{N} x_i}{dxdydt} \\ \frac{\sum_{i=1}^{N} y_i}{dxdydt} \end{pmatrix}, \tag{12}$$

where x_i and y_i are the distances traveled in A in direction x, respectively y by pedestrian i. The velocity in direction x (or y) is defined as the average distance traveled in x direction (or in y direction) divided by the total time spent

$$\vec{\boldsymbol{v}}(A) = \begin{pmatrix} v_x(A) \\ v_y(A) \end{pmatrix} = \begin{pmatrix} \frac{\sum_{i=1}^{N} x_i}{\sum_{i=1}^{N} t_i} \\ \frac{\sum_{i=1}^{N} y_i}{\sum_{i=1}^{N} t_i} \end{pmatrix}. \tag{13}$$

At the limit $dt \to 0$, the density converges to the number of pedestrians present in $[dx \times dy]$ at a specific moment in time. At the limit $dx \to 0$ ($dy \to 0$) flow converges to the number of pedestrians per unit of time and per unit of length. In the rest of the paper, we refer to this method as the XY-T method.

Another approach is provided by Helbing et al. (2007). This method defines the characteristics at any point (x, y) by weighting the relative influence of the surrounding pedestrians using Gaussian distance-dependent weight function

$$f\left(\begin{pmatrix} x_i(t) \\ y_i(t) \end{pmatrix} - \begin{pmatrix} x \\ y \end{pmatrix}\right) = \frac{1}{\pi R^2} \exp\left(- \frac{\left\| \begin{pmatrix} x_i(t) \\ y_i(t) \end{pmatrix} - \begin{pmatrix} x \\ y \end{pmatrix} \right\|^2}{R^2} \right), \tag{14}$$

where R represents the distance up-to-which the influence of pedestrians is taken into account, and $(x_i(t), y_i(t))^T$ the location of pedestrian i. The density is defined as

$$k(x, y, t) = \sum_i f\left(\begin{pmatrix} x_i(t) \\ y_i(t) \end{pmatrix} - \begin{pmatrix} x \\ y \end{pmatrix}\right). \tag{15}$$

The velocity is given by

$$\vec{\boldsymbol{v}}(x, y, t) = \frac{\sum_i \vec{\boldsymbol{v}}_i(t) f\left(\begin{pmatrix} x_i(t) \\ y_i(t) \end{pmatrix} - \begin{pmatrix} x \\ y \end{pmatrix}\right)}{\sum_i f\left(\begin{pmatrix} x_i(t) \\ y_i(t) \end{pmatrix} - \begin{pmatrix} x \\ y \end{pmatrix}\right)}, \tag{16}$$

where $\vec{\boldsymbol{v}}_i(t)$ is the velocity of pedestrian i at time t, which is given by (8). The flow is determined using the fundamental flow Eq. (10). In the rest of the paper, we refer to this method as the exponentially weighted distance method (EW), as in Duives et al. (2015).

Steffen and Seyfried (2010) propose the method in which the spatial discretization is adjusted to the data through the use of Voronoi diagrams (Okabe et al., 2000). The Voronoi space decomposition assigns a personal region A_i to each pedestrian i, in such a way that each point in the personal region is closer to i than to any other pedestrian, with respect of the Euclidean distance. The density at position (x, y) at time t is defined as

$$k(x, y, t) = \frac{1}{|A_i|}, \quad \text{for} \quad (x, y) \in A_i, \tag{17}$$

where $|A_i|$ is the area of A_i. The velocity is defined based on position differences of pedestrian i between time instances t_1 and t_2

$$\vec{\boldsymbol{v}}(x, y, t) = \frac{\begin{pmatrix} x_i(t_2) \\ y_i(t_2) \end{pmatrix} - \begin{pmatrix} x_i(t_1) \\ y_i(t_1) \end{pmatrix}}{t_2 - t_1}, \quad \text{for} \quad (x, y) \in A_i, \tag{18}$$

where $(x_i(t), y_i(t))^T$ is the location of pedestrian i at time t. Time instances t_1 and t_2 are determined such that the effect of the swaying movement of pedestrians is reduced, which requires an extensive pre-processing of each pedestrian trajectory (Duives, 2012). The flow within an interval is defined using fractional counts obtained from Voronoi cells: half a person has passed a segment if half of the Voronoi cell has passed it. For more details we refer to Steffen and Seyfried (2010). In the rest of the paper, we refer to this method as the Voronoi-based method (VB), as in Duives et al. (2015).

There also exist headway-based approaches for the definition of density variable, such as Harmonically Weighted Mean Distance and Minimum Distance, both with or without a vision field taken into account. According to Duives et al. (2015),

Please cite this article in press as: Nikolić, M., Bierlaire, M. Data-driven spatio-temporal discretization for pedestrian flow characterization. Transport. Res. Part C (2017), http://dx.doi.org/10.1016/j.trc.2017.08.026

these approaches are not capable of providing correct and consistent estimation and are therefore excluded from the further analysis in our study.

2.2.2. Comparison of methods

A summary of general characteristics of the approaches is provided in Table 1. We first compare the approaches in terms of the scale that is considered, that is in terms of whether the characterization is defined by using the information about a single pedestrian (microscopic) or multiple pedestrians (macroscopic). Then, the analysis is made with respect to the exact way the spatial and temporal aggregation is performed at a given scale. Finally, the approaches are contrasted in terms of the type of data required to perform the characterization.

Most of the methods (XY-T, GB, RB, EW) rely on macroscopic approach. This approach does not always comply with the nature of the underlying system. Pedestrians differ in many ways (Weidmann, 1993; Bierlaire and Robin, 2009) and studying pedestrian movement at the macroscopic level may lead to the loss of heterogeneity. Also, by using macroscopic definitions, velocity and flow vectors may nullify if the pedestrians do not all move in the same direction. As for the XY-T method, van Wageningen-Kessels et al. (2014) state that "if about half of the pedestrians walks from left to right, and the rest walks in the other direction, this causes the flows and velocities in x direction to (almost) cancel out". The same example can be used to conclude that the GB, the RB and the EW method suffer from the same issue. On the other hand, microscopic characterization (employed in the VB method) is able to reflect these particularities of pedestrian traffic. It is further supported by detailed movement data (at the individual level) that is more and more available due to the advances in tracking technologies (Bauer et al., 2009). The microscopic approach is characterized by higher computational burden, which becomes less problematic in the era of high-performance computers.

All the approaches have in common the arbitrary chosen temporal intervals for the specification of velocity and flow indicators. Most of them (XY-T, GB, RB, EW) additionally depend on an arbitrary spatial aggregation. These may generate noise in the data and the results may be highly sensitive to minor changes. The choice of the shape, size and locations of the spatial units in the methods XY-T, GB and RB influences the results significantly (Steffen and Seyfried, 2010). Also, the use of fixed aggregation over time might cause large fluctuations in the indicator values when pedestrians cross the boundaries of the aggregation units. An additional level of arbitrariness is introduced when a pedestrian is exactly at the border between two units, and an arbitrary decision must be made about what unit she belongs to (Duives et al., 2015). Indicators obtained using the EW approach strongly depend on the radius R and, in general, on the choice of the influence function f, given by (14). The VB method of Steffen and Seyfried (2010) is the only one that addresses the issue of arbitrary aggregation in space through a data-driven approach. The spatial units in this approach are not fixed over time. Aggregation follows the trend of the data by computing Voronoi diagrams for every time step. The issue is that Voronoi diagram is potentially not enclosed. There is no clear understanding about where to put the Voronoi boundaries in directions where no other pedestrians are present. Steffen and Seyfried (2010) use a restriction of the individual cells in size ($2m^2$) to deal with this issue, which is active only for a few cells.

An analytical description of the trajectories is required for the XY-T method. Consequently, interpolation has to be used when sampled data is available, which is another source of errors. The methods GB, RB, EW and VB can be applied on trajectories described either analytically or as a sample of points. Note that these approaches require a tracking technology that produces synchronized samples. Often, the cameras used to track pedestrians in a distributed network of cameras operate with different sampling frequency or produce observations at irregular intervals. In this case not all trajectories have observations at the same time instants, which might lead to the underestimation of the indicators. It is therefore necessary to perform the interpolation of trajectories when using non-synchronized samples, before applying the methods.

The methodology proposed in this article is similar to the approach used in Jabari et al. (2014). It relies on the microscopic definitions of Edie (1963) adopted for pedestrian traffic, and extended through a data-driven discretization framework. Our preliminary ideas regarding the proposed methodology are discussed in Nikolić and Bierlaire (2014, 2015).

Table 1
Characteristics of the approaches.

Method	Scale	Spatial aggregation		Temporal aggregation		Data type
		Unit	Assumptions	Unit	Assumptions	
XY-T	Macroscopic	Area	Shape Size Location	Interval	Duration	Trajectories
Grid-based (GB)	Macroscopic	Cell	Size Location	Interval	Duration	Trajectories Sync. sample
Range-based (RB)	Macroscopic	Circle	Radius Location	Interval	Duration	Trajectories Sync. sample
Exponentially-weighted (EW)	Macroscopic	Range	Influence function Range of influence	Interval	Duration	Trajectories Sync. sample
Voronoi-based (VB)	Microscopic	Voronoi cell	Boundary conditions	Interval	Duration	Trajectories Sync. sample

Please cite this article in press as: Nikolić, M., Bierlaire, M. Data-driven spatio-temporal discretization for pedestrian flow characterization. Transport. Res. Part C (2017), http://dx.doi.org/10.1016/j.trc.2017.08.026

3. Preliminaries

We consider a space-time representation and denote the area of interest by $\Omega \subset \mathbb{R}^3$. An orthonormal basis of this space is considered. The distance along each of the two spatial axes is expressed in meters, and the unit for time is seconds. The triplet $p = (p_x, p_y, p_t) = (x, y, t) \in \Omega$ represents a physical position (x, y) in space at a specific time t. It is assumed that Ω is convex, that is obstacle-free, and bounded.

The trajectory of pedestrian i is a curve in space and time. It is a set of points

$$\Gamma_i : \{p_i(t) | p_i(t) = (x_i(t), y_i(t), t)\}, \tag{19}$$

indexed by time t that spans the horizon of the analysis, and $x_i(t)$ and $y_i(t)$ are the coordinates of the position of pedestrian i at time t.

In practice, the analytical description of a trajectory is seldom available. Instead, the pedestrian trajectory data is collected through an appropriate tracking technology (Alahi et al., 2014a, 2011; Daamen and Hoogendoorn, 2003). In this case time is discretized and the trajectory is described as a finite collection of triplets (a sample of points)

$$\Gamma_i : \{p_{is} | p_{is} = (x_{is}, y_{is}, t_s)\}, \tag{20}$$

where $s = [1, 2, \ldots, T_i]$ and $t_s = [t_1, t_2, \ldots, t_{T_i}]$ correspond to the available sample.

The speed along the continuous trajectory of pedestrian i is given by

$$v_i(t) = (x_i'(t), y_i'(t), 1). \tag{21}$$

Interpolation methods or finite differences (forward, backward or central) approximation can be used with sampled data.

4. Methodology

This section is organized in four parts. The first part presents the derivation of the spatio-temporal discretization framework using a data-driven approach. In the second part, we define pedestrian traffic variables, that is density, flow and velocity. The variables are defined by revising the existing microscopic definitions according to the proposed discretization (as motivated in Section 2). In the third part, we present concrete suggestions for the operationalization of the general and abstract concepts related to the discretization framework. The last part focuses on the implementation details.

4.1. Data-driven discretization

We propose the discretization in space and time that is defined based on three-dimensional (3D) Voronoi diagrams associated with pedestrian trajectories. We call the set of trajectories the generator set $\Gamma = \{\Gamma_1, \ldots, \Gamma_n\}$, consistently with the literature. We assume that elements in Γ do not intersect each other. This assumption is reasonable, as two pedestrians cannot be at the exact same place at the exact same time. The main idea for defining the partition of Ω is that (i) every point $p \in \Omega$ belongs to a unique discretization unit, (ii) each discretization unit is assigned to one generator $\Gamma_i \in \Gamma$ according to a certain assignment rule and (iii) the resulting discretization units associated with the trajectories are collectively exhaustive and mutually exclusive. Therefore, the partitioning is characterized by the assignment of each point $p \in \Omega$ to one generator from Γ. The discretization units are then defined as the set of points p assigned to the same generator.

Given a non-empty space Ω and a generator set Γ, the assignment rule δ_Γ of a point $p \in \Omega$ to an element of Γ is in the literature (Okabe et al., 2000) often specified in terms of distance relations D (not necessary distance metric). The point p is assigned to the "closest" generator in term of a given distance

$$\delta_\Gamma(p, \Gamma_i) = \begin{cases} 1, & D(p, \Gamma_i) \leqslant D(p, \Gamma_j), \quad \forall j \neq i \\ 0, & \text{otherwise}. \end{cases} \tag{22}$$

Note that this rule is ambiguous for points p that are equidistant to two trajectories. In this case, an additional arbitrary rule must be used. For instance, if $D(p, \Gamma_i) = D(p, \Gamma_j)$, then it can be decided that p is assigned to Γ_i if $i < j$.

If the generators are continuous trajectories (19), the distance may be defined as

$$D(p, \Gamma_i) = \min_t \{d(p, p_i(t)) | p_i(t) \in \Gamma_i, \Gamma_i \in \Gamma, p \in \Omega\}, \tag{23}$$

where $d(p, q)$ is the distance between two points p and q in Ω. Concrete examples of this distance function are discussed in Section 4.3. Similarly, if the generators are sampled (20), the distance may be defined as

$$D(p, \Gamma_i) = \min_s \{d(p, p_{is}) | p_{is} \in \Gamma_i, \Gamma_i \in \Gamma, p \in \Omega\}. \tag{24}$$

Under the assignment rule (22), we consider the set of points V_i assigned to Γ_i

$$V_i = \{p | \delta_\Gamma(p, \Gamma_i) = 1, p \in \Omega, \Gamma_i \in \Gamma\}, \tag{25}$$

which represents a personal spatio-temporal region associated with pedestrian i. For each i, V_i is a convex subset of Ω called a Voronoi cell. Collectively, they represent a Voronoi diagram. The assumption that Ω is obstacle-free and bounded (Section 3) allows for the creation of non-degenerate Voronoi diagrams

Please cite this article in press as: Nikolić, M., Bierlaire, M. Data-driven spatio-temporal discretization for pedestrian flow characterization. Transport. Res. Part C (2017), http://dx.doi.org/10.1016/j.trc.2017.08.026

$$\mathcal{V} = \{V_1, \ldots, V_n\}, \tag{26}$$

generated by Γ.

In a three-dimensional space Ω the plane through the point $p_0 = (x_0, y_0, t_0)$ and with non-zero normal vector $\vec{\boldsymbol{n}} = (a, b, c)$ has equation

$$\mathcal{P}_{\vec{\boldsymbol{n}},p_0} : ax + by + ct + d = 0, \tag{27}$$

where $d = -ax_0 - by_0 - ct_0$. We define the set of points $A(V_i, \mathcal{P}_{\vec{\boldsymbol{n}},p_0})$ corresponding to the intersection of the cell V_i and the plane $\mathcal{P}_{\vec{\boldsymbol{n}},p_0}$

$$A(V_i, \mathcal{P}_{\vec{\boldsymbol{n}},p_0}) = \{p | p \in \{V_i \cap \mathcal{P}_{\vec{\boldsymbol{n}},p_0}\}\}. \tag{28}$$

For $\vec{\boldsymbol{n}} = (0, 0, 1)$ we have a plane parallel to the $x - y$ plane and its intersection with V_i is given as

$$A(V_i, \mathcal{P}_{(0,0,1),p_0}) = \{p | p \in V_i \quad \text{and} \quad p_t = t_0\}. \tag{29}$$

It represents a set of dimension 2 or a physical area on the floor (illustrated in Fig. 1(left)), at time t_0. The area of this cell is denoted by $|A(V_i, \mathcal{P}_{(0,0,1),p_0})|$, with the unit in m^2. Similarly, for $\vec{\boldsymbol{n}} = (a, b, 0)$ we have

$$A(V_i, \mathcal{P}_{(a,b,0),p_0}) = \{p | p \in V_i \quad \text{and} \quad ap_x + bp_y = ax_0 + by_0\}. \tag{30}$$

It is the set of dimension 2 or a segment on the floor occupied by pedestrian i in the direction perpendicular to $\vec{\boldsymbol{n}} = (a, b, 0)$ during the time interval spanning V_i. The area of the cell is denoted by $|A(V_i, \mathcal{P}_{(a,b,0),p_0})|$, with the unit in ms. Note that if $\vec{\boldsymbol{n}} = (1, 0, 0)$ and $\vec{\boldsymbol{n}} = (0, 1, 0)$, the corresponding planes are parallel to the $x - t$, respectively the $y - t$ plane (illustrated in Fig. 1(right)).

4.2. Definitions of pedestrian traffic variables

Assume that the Voronoi cell V_i is associated with position $(x, y, t) \in \Omega$. The density at (x, y, t) is defined as the inverse of the area of the set $A(V_i, \mathcal{P}_{(0,0,1),(x,y,t)})$ assigned to pedestrian i at time t

$$k(x, y, t) = \frac{1}{|A(V_i, \mathcal{P}_{(0,0,1),(x,y,t)})|}, \tag{31}$$

where $A(V_i, \mathcal{P}_{(0,0,1),(x,y,t)})$ is given by (29) and $|A(V_i, \mathcal{P}_{(0,0,1),(x,y,t)})|$ is the area of this set. The location (x, y) determines pedestrian i and the corresponding set $A(V_i, \mathcal{P}_{(0,0,1),(x,y,t)})$. The unit of $k(x, y, t)$ is a number of pedestrians per square meter. This definition is consistent with (11), adapted to this 3D Voronoi context.

The flow in the direction determined by the vector $\vec{\boldsymbol{e}} = (a, b)$ is defined as the inverse of the area of the set $A(V_i, \mathcal{P}_{(a,b,0),(x,y,t)})$ assigned to pedestrian i

$$\vec{\boldsymbol{q}}_e(x, y, t) = \frac{1}{|A(V_i, \mathcal{P}_{(a,b,0),(x,y,t)})|}, \tag{32}$$

where $A(V_i, \mathcal{P}_{(a,b,0),(x,y,t)})$ is given by (30) and $|A(V_i, \mathcal{P}_{(a,b,0),(x,y,t)})|$ is the area of this set. The point (x, y, t) determines pedestrian i and the corresponding set $A(V_i, \mathcal{P}_{(a,b,0),(x,y,t)})$. The set $(V_i, \mathcal{P}_{(a,b,0),(x,y,t)})$ belongs to the spatio-temporal domain. Therefore, the

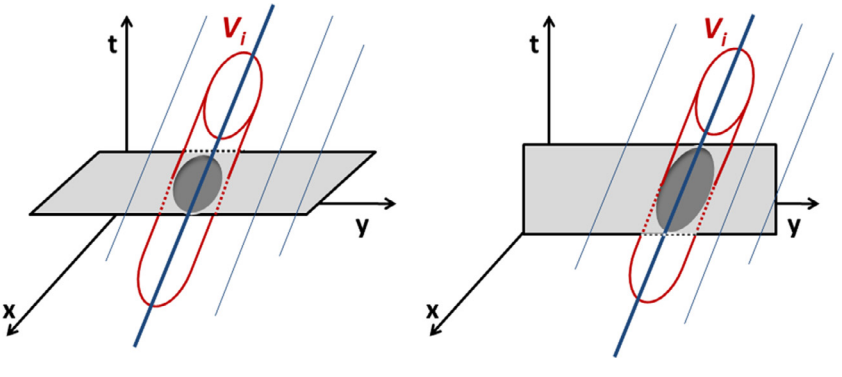

Fig. 1. 3D Voronoi-based discretization: set $A(V_i, \mathcal{P}_{(0,0,1),p_0})$ (left), set $A(V_i, \mathcal{P}_{(0,1,0),p_0})$ (right).

Please cite this article in press as: Nikolić, M., Bierlaire, M. Data-driven spatio-temporal discretization for pedestrian flow characterization. Transport. Res. Part C (2017), http://dx.doi.org/10.1016/j.trc.2017.08.026

unit of $\vec{\boldsymbol{q}}_e(x,y,t)$ is a number of pedestrians per meter per second. The flow in x and y directions is obtained considering the inverse of the areas $|A(V_i,\mathcal{P}_{(1,0,0),(x,y,t)})|$ and $|A(V_i,\mathcal{P}_{(0,1,0),(x,y,t)})|$, consistently with (12).

Adopting the usual definition of the velocity (the ratio between the flow and density), from (31) and (32) we have

$$\vec{\boldsymbol{v}}_e(x,y,t)=\frac{\vec{\boldsymbol{q}}_e(x,y,t)}{k(x,y,t)}=\frac{|A(V_i,\mathcal{P}_{(0,0,1),(x,y,t)})|}{|A(V_i,\mathcal{P}_{(a,b,0),(x,y,t)})|}. \tag{33}$$

It represents the mean speed of pedestrian i (Jabari et al., 2014) in the direction determined by the vector $\vec{\boldsymbol{e}}=(a,b)$, expressed in meters per second. Note that the framework allows for the specification and measurement of the indicators $\vec{\boldsymbol{q}}_e(x,y,t)$and $\vec{\boldsymbol{v}}_e(x,y,t)$ in any direction $\vec{\boldsymbol{e}}$ of interest.

The proposed definitions (31)–(33) are independent from arbitrarily chosen intervals in space and time, due to the fact that they rely on a data-driven discretization. Our approach is microscopic and therefore suitable for multi-directionl nature of pedestrian flows and able to preserve the heterogeneity of pedestrians (Jabari et al., 2014). The issues characteristic for the macroscopic approach, discussed in Section 2, do not appear at the microscopic level. Also, the proposed definitions can be applied on continuous or sampled trajectories. The samples, in general, do not need to be synchronized.

We refer to the proposed approach as the *3D Voronoi characterization* (3DVoro).

4.3. Spatio-temporal distances

The proposed framework is fairly general, and can accommodate various methods to generate the Voronoi diagrams, based on different definitions of the distance between two points. To construct 3D Voronoi diagrams (Section 4.1), we need to define the exact form of the distance relation d used in (23) and (24). Applying the Euclidean distance in $\mathbb{R}^3$ looks like a natural choice. However, it is important to keep in mind that it would mix units in square meters with units in seconds. We propose here several ways to deal with it. First, we propose to restrict the Euclidean distance in the spatial dimension, and consider each point in time as independent. Second, we propose distances in $\mathbb{R}^3$ that convert seconds into meters using speed. Third, we account for the pedestrian dynamics to define the distance, anticipating her future position. Finally, we define a distance through the identification of points that are equidistant. Their respective performance is empirically evaluated in Section 5.

We denote by $p=(x,y,t)$ a point from Ω. An observation from the trajectory of pedestrian i is denoted by $p_i=(x_i,y_i,t_i)$. It refers to either $p_i(t)$ or p_{is}, depending on the context.

4.3.1. Spatial Euclidean distance

The first distance that we propose is defined with respect to the standard Euclidean distance in the spatial dimension, that is

$$d_E(p,p_i)=\begin{cases}\sqrt{(x-x_i)^2+(y-y_i)^2}, & t=t_i\\ \infty, & \text{otherwise.}\end{cases} \tag{34}$$

Intuitively, each point in time is independent. This is motivated by the availability of snapshots of the floor area at given points in time. This implies that all pedestrians in the area must be observed at the exact same time.

We refer to the characterization obtained using this distance as the *Euclidean 3D Voronoi characterization* (E-3DVoro).

4.3.2. Time-transform distances

We define the set of three distances that apply a conversion parameter, expressed in meters per second, to transform the temporal difference between the points into the spatial one. They are denoted as the Time-Transform distances $(d_{TT_1},d_{TT_2},d_{TT_3})$. The distances differ in terms of the choice of the conversion parameter and in the way of coupling the spatial and temporal component. They are defined as

$$d_{TT_1}(p,p_i)=\sqrt{(x-x_i)^2+(y-y_i)^2+v^2(t-t_i)^2}, \tag{35}$$

where v is a parameter representing the typical speed of pedestrians (a value of v = 1.34 m/s is used in our experiments, Weidmann (1993)),

$$d_{TT_2}(p,p_i)=\sqrt{(x-x_i)^2+(y-y_i)^2+\hat{v}_i(t_i)^2(t-t_i)^2}, \quad \text{and} \tag{36}$$

$$d_{TT_3}(p,p_i)=\sqrt{(x-x_i)^2+(y-y_i)^2}+\hat{v}_i(t_i)|t-t_i|, \tag{37}$$

where $\hat{v}_i(t_i)$ is the speed at time t_i on trajectory Γ_i. The choice of the conversion parameter $\hat{v}_i(t_i)$ in (36) and (37) allows to treat moving pedestrians in a different way than standing pedestrians.

Please cite this article in press as: Nikolić, M., Bierlaire, M. Data-driven spatio-temporal discretization for pedestrian flow characterization. Transport. Res. Part C (2017), http://dx.doi.org/10.1016/j.trc.2017.08.026

The distances (35) and (36) combine the spatial and temporal components based on the Euclidean norm, using two different values for the speed. In (37), the components are considered as independent and kept separately. The distance d_{TT_3} is defined as a weighted sum of two norms. When $t = t_i$, all distances are equivalent to (34).

We refer to the characterization obtained using these three distances as the *Time-Transform 3D Voronoi characterization* (TT_1-3DVoro, TT_2-3DVoro and TT_3-3DVoro).

4.3.3. Predictive distance

The predictive distance anticipates the forward movement of pedestrians. The anticipated positions x_i^a and y_i^a are extrapolated from the current velocities of pedestrians for a time determined by the anticipation time $t - t_i$

$$x_i^a = x_i^a(t) = x_i + (t - t_i)\, v_i^x(t_i), \tag{38}$$

$$y_i^a = y_i^a(t) = y_i + (t - t_i)\, v_i^y(t_i), \tag{39}$$

where $v_i^x(t_i)$ and $v_i^y(t_i)$ are the speed of pedestrian i at t_i in x, respectively y, direction.

The distance is specified as

$$d_P(p, p_i) = \begin{cases} \sqrt{(x_i^a - x)^2 + (y_i^a - y)^2}, & t - t_i \geqslant 0 \\ \infty, & \text{otherwise.} \end{cases} \tag{40}$$

Note that it is not a metric distance, as it is not symmetric. The anticipation time extends from zero to a positive value ($t - t_i$). Points p that are backward in time with respect to the current positions of pedestrian are considered infinitely distant. When $t = t_i$, the distance reduces to the standard $\mathbb{R}^2$ Euclidean distance. The consideration of individual speeds allows for the distinction between pedestrians that perform movement from those that stand.

We refer to the characterization obtained using this distance as the *Predictive 3D Voronoi characterization* (P-3DVoro).

4.3.4. Mahalanobis distance

The Mahalanobis distance is specified as

$$d_M(p, p_i) = \sqrt{(p - p_i)^T \boldsymbol{M}_i (p - p_i)}, \tag{41}$$

where $\boldsymbol{M}_i$ is a change of variable matrix. It is a symmetric, positive-definite matrix, which defines how the distances are measured in different spatio-temporal directions from the perspective of pedestrian i. To implement this distance we need to determine the matrix $\boldsymbol{M}_i$. We do so by identifying 6 points in Ω such that they are equidistant to p_i for the Mahalanobis distance. We take into account the information about the speed and direction of pedestrians, in the sense that the points that are in the movement direction of a pedestrian are "closer" than the points from other directions.

Formally, we consider three directions of interest. First, we define the normalized direction of movement in the space-time dimensions

$$d^1(t_i) = \frac{v_i(t_i)}{||v_i(t_i)||}, ||d^1(t_i)|| = 1, \tag{42}$$

where $v_i(t_i)$ is the speed along the trajectory of pedestrian i given by (21). We next define a normalized spatial direction orthogonal to $d^1(t_i)$, that is

$$d^2(t_i) = \begin{pmatrix} d_x^1(t_i) \\ d_y^2(t_i) \\ 0 \end{pmatrix}, \tag{43}$$

such that $d^1(t_i)^T d^2(t_i) = 0$ and $||d^2(t_i)|| = 1$. The third direction is for time

$$d^3(t_i) = \begin{pmatrix} 0 \\ 0 \\ \Delta t \end{pmatrix}, \tag{44}$$

where Δt is typically determined by the sampling frequency and $||d^3(t_i)|| = \Delta t$.

We determine the matrix $\boldsymbol{M}_i$, and the distance d_M, such that the following points in the defined directions are all at distance α from the point p_i. The key feature is that, in the direction of movement, the distances do not refer to the position at time t, but the positions at time $t + \Delta t$ and $t - \Delta t$. The points S_1 and S_2 in the d^1 direction are at α and $-\alpha$ from the positions at time $t + \Delta t$, respectively $t - \Delta t$

$$S_1(t_i, \alpha) = p_i + \Delta t\, v_i(t_i) + \alpha d^1(t_i), \tag{45}$$

$$S_2(t_i, \alpha) = p_i - \Delta t\, v_i(t_i) - \alpha d^1(t_i). \tag{46}$$

Please cite this article in press as: Nikolić, M., Bierlaire, M. Data-driven spatio-temporal discretization for pedestrian flow characterization. Transport. Res. Part C (2017), http://dx.doi.org/10.1016/j.trc.2017.08.026

In the direction d^2 we consider the point S_3 that is at α from the point p_i

$$S_3(t_i, \alpha) = p_i + \alpha d^2(t_i), \tag{47}$$

and the point S_4 that is at $-\alpha$ from the point p_i

$$S_4(t_i, \alpha) = p_i - \alpha d^2(t_i). \tag{48}$$

Similarly, in time direction d^3 we consider the point S_5 that is at α from the point p_i

$$S_5(t_i, \alpha) = p_i + \alpha d^3(t_i), \tag{49}$$

and the point S_6 that is at $-\alpha$ from the point p_i

$$S_6(t_i, \alpha) = p_i - \alpha d^3(t_i). \tag{50}$$

This is illustrated in Fig. 2.

In standard Euclidean space we have that

$$||S_1(t_i, \alpha) - p_i|| = ||S_2(t_i, \alpha) - p_i|| = \Delta t||v_i(t_i)|| + \alpha. \tag{51}$$

It shows that, in the direction d^1, the forward and backward distances are stretched by the quantity $\Delta t||v_i(t_i)||$. This is designed to anticipate the movement of pedestrians and to overcome the lack of continuous observations when dealing with samples of points. The additional term vanishes when $\Delta t \to 0$. The approach also allows to deal with moving and standing pedestrians in a different way. The distance in the d^2 direction is consistent with Euclidean distance

$$||S_3(t_i, \alpha) - p_i|| = ||S_4(t_i, \alpha) - p_i|| = ||\alpha d^2(t_i)|| = \alpha. \tag{52}$$

The distance in time direction d^3 is proportional to the time discretization

$$||S_5(t_i, \alpha) - p_i|| = ||S_6(t_i, \alpha) - p_i|| = ||\alpha d^3(t_i)|| = \alpha \Delta t. \tag{53}$$

In particular, it shrinks to zero when $\Delta t \to 0$.

In our experiments, a value of $\alpha = 1$ is used.

We refer to the characterization obtained using this distance as the *Mahalanobis 3D Voronoi characterization* (M-3DVoro).

4.4. Implementation details

The Voronoi diagrams for higher order generators (such as curves) in higher dimensions are difficult to compute in an exact way (Hoff et al., 1999). For a number of applications an approximation of the exact diagram is considered (Schueller, 2007; Rong and Tan, 2007; Park et al., 2006; Fuchida et al., 2005).

We also use an approximate algorithm for the implementation of the Voronoi diagram detailed in Section 4.1. The area of interest, Ω, is discretized into regular cells. The cells are used in the assignment rule (22), instead of points p. In the literature, this approximation is known as the Naïve algorithm (Van der Putte, 2009).

The presented algorithm is merely one possibility. It is intuitive, but does not feature high computational efficiency. To improve the efficiency of the algorithm, specialized data structures can be considered (e.g. kd-tree), as discussed in Rigaux et al. (2001). However, the aim of our study is to illustrate the performance of the proposed methodology, and not to contribute to the field of computational geometry. The analysis of other algorithms to construct Voronoi diagrams is therefore out of the scope of this paper.

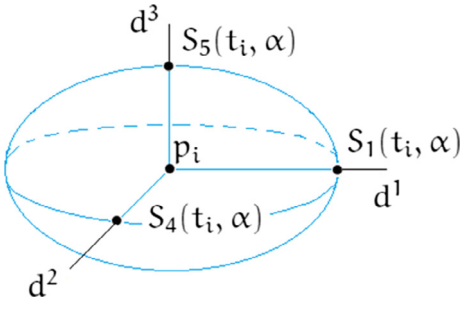

Fig. 2. Mahalanobis distance – illustration.

Please cite this article in press as: Nikolić, M., Bierlaire, M. Data-driven spatio-temporal discretization for pedestrian flow characterization. Transport. Res. Part C (2017), http://dx.doi.org/10.1016/j.trc.2017.08.026

5. Empirical analysis

The performance of our approach is evaluated based on synthetic data that is generated using the NOMAD simulation tool (Campanella et al., 2014; Hoogendoorn and HL Bovy, 2003). The flow is simulated in a 4 m by 4 m area, during 10 s for unidirectional (*Uni*) flow composition. The data is generated for two different scenarios. In the first scenario, we consider lower demand (1.2 pedestrians per second) and homogeneous pedestrian population ($LD - HomoPop$). The homogeneity of the population is reflected through (approximately) homogenous walking speed of pedestrians. We use the average speed value of 1.34 m/s, according to the study of Weidmann (1993). In the second scenario, we consider higher demand (3.6 pedestrians per second) and heterogeneous pedestrian population ($HD - HeteroPop$). To represent the heterogeneity in the population, we consider three sub-populations (slow, average and fast) with respective speeds of 0.5 m/s, 1.3 m/s and 2.1 m/s. Each sub-population has roughly the same size.

Our objective is to analyze the robustness of the approach with respect to the simulation noise (Section 5.1) and with respect to the sampling frequency (Section 5.2). The performance of the 3DVoro method (for all the distances) is compared with the performance of the XY-T and VB methods. The consideration of these two methods is motivated by the empirical comparisons of the existing approaches presented in Duives et al. (2015), where it has been concluded that the XY-T and VB methods perform the best. In the application of the XY-T method, the parameters of the cells A reported in Duives et al. (2015) are used: a time interval of 1 s, and a grid cell size of 1×1 m. Note that, the VB method corresponds to the E-3DVoro when used for the discrete time instants to discretize the spatial dimension only. Therefore, the VB method will not be considered separately.

5.1. Robustness with respect to the simulation noise

In this section we analyze the performance of the approach when frequent pedestrian observations are available. For this purpose we consider the trajectories obtained from NOMAD for minimal trajectory step (0.1 s). In the case of the XY-T method, the distances traveled and the times spent by pedestrians in regions A (Section 2.2) are obtained using interpolation.

We synthesize 100 sets of pedestrian trajectories for each scenario and evaluate the variance of the indicators across these replications. The described settings of the simulator remain unchanged for a given scenario. The indicators (k, v, q) are calculated for each set of the trajectories via 3DVoro (for all the distances) and the XY-T method. The methods are compared based on the standard deviation of the indicators at specific points due to simulation noise.

Let M represent the method (3DVoro or XY-T), r a realization of NOMAD simulation ($r = 1, \ldots, 100$) and p a point from Ω. We denote by $\theta_r^M(p) = (k_r^M(p), v_r^M(p), q_r^M(p))$ a vector of indicators at point p obtained by applying the method M to the r^{th} set of trajectories. For each method we calculate the standard deviation of the indicators at p as

$$\sigma_R^M(p) = \sqrt{\frac{1}{R}\sum_{r=1}^{R}\left(\theta_r^M(p) - \mu_R^M(p)\right)^2}, \tag{54}$$

where $\mu_R^M(p) = \frac{1}{R}\sum_{r=1}^{R}\theta_r^M(p)$ and $R = 100$. This procedure is repeated for 1000 randomly selected points p (these points are the same across simulation). The results are reported using boxplot representation in Fig. 3 for $Uni_{LD-HomoPop}$, and in Fig. 4 for $Uni_{HD-HeteroPop}$.

The standard deviations of the indicators are larger for $Uni_{HD-HeteroPop}$ for all the methods, compared to $Uni_{LD-HomoPop}$. This can be explained by the larger changes in the data due to higher complexity of the system in $Uni_{HD-HeteroPop}$. However, a similar trend is noticeable in the results for both scenarios.

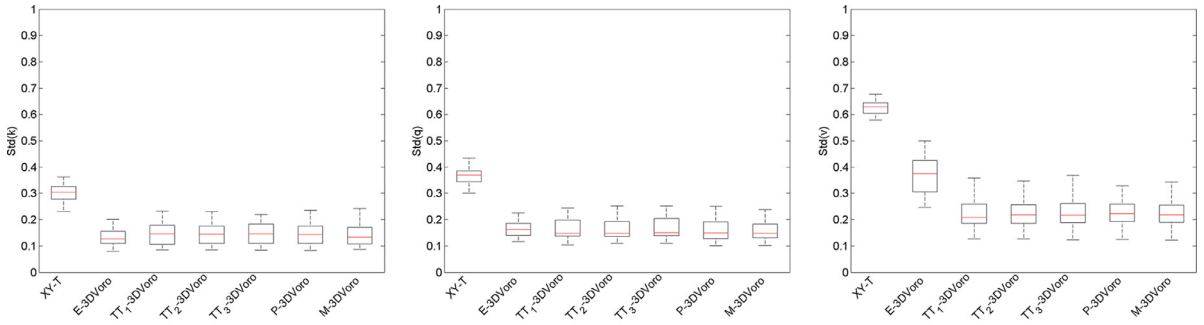

(a) Standard deviation of density indicator; (b) Standard deviation of flow indicator; (c) Standard deviation of velocity indicator;

Fig. 3. Robustness to the simulation noise – $Uni_{LD-HomoPop}$.

Please cite this article in press as: Nikolić, M., Bierlaire, M. Data-driven spatio-temporal discretization for pedestrian flow characterization. Transport. Res. Part C (2017), http://dx.doi.org/10.1016/j.trc.2017.08.026

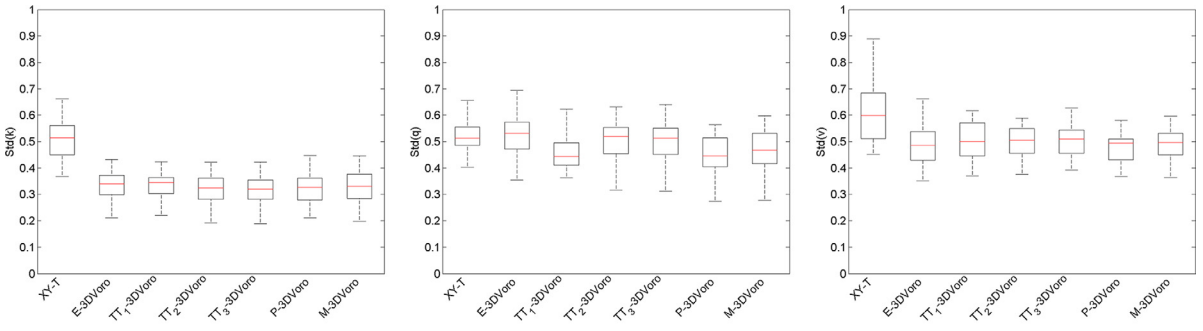

(a) Standard deviation of density indicator; (b) Standard deviation of flow indicator; (c) Standard deviation of velocity indicator;

Fig. 4. Robustness to the simulation noise – $Uni_{HD-HeteroPop}$.

The results for the density indicator (Figs. 3(a) and 4(a)), and for the flow indicator (Figs. 3(b) and 4(b)), are similar across different 3DVoro distances for both scenarios. In the case of speed, E-3DVoro exhibits larger standard deviations as compared to other 3DVoro methods for $Uni_{LD-HomoPop}$ (Fig. 3(c)). This suggests that 3DVoro with distances that account for the speed and/or movement direction of pedestrians lead to lower variance in the results when demand is low. When demand is higher (Fig. 4(c)), higher number of pedestrian trajectories leads to similar behavior of different distances, and consequently to similar results.

In comparison to 3DVoro approach, in the XY-T method the simulation noise is significantly amplified. The results suggest that the changes of trajectories, even though for the same simulated settings, dramatically affect the measured indicators of the XY-T method.

5.2. Robustness with respect to the sampling frequency

In order to evaluate the effectiveness of the approach when sampled data is available, we consider the samples of points from the synthetic trajectories. The samples are obtained using different sampling frequencies (3 s^{-1}, 2 s^{-1}, 1 s^{-1} and 0.5 s^{-1}), as illustrated in Fig. 5. The feature of interest is the robustness of the approach with respect to the sampling frequency. That is, the ability of the approach to produce stable results even in the lack of frequent observations.

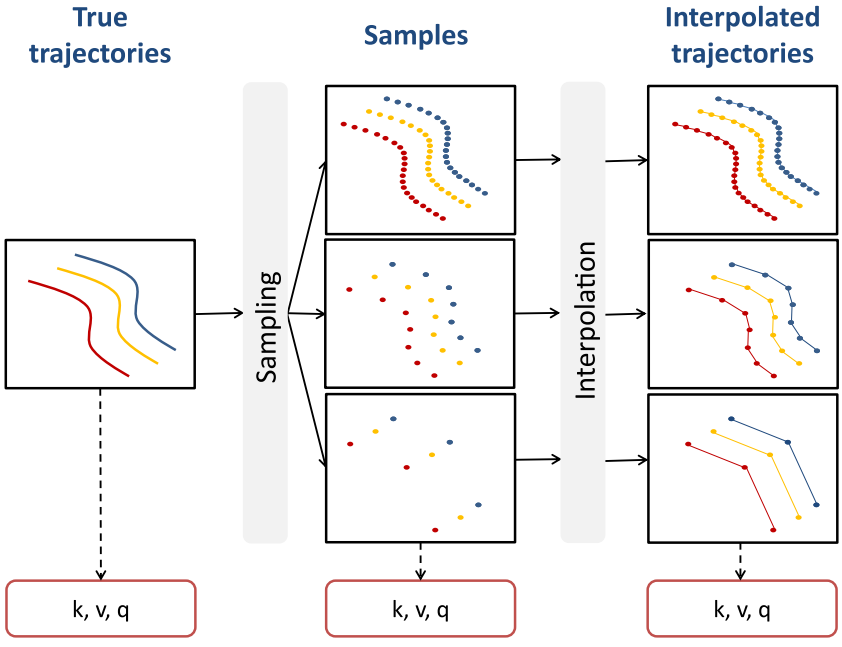

Fig. 5. Sampling of trajectories and interpolation.

Please cite this article in press as: Nikolić, M., Bierlaire, M. Data-driven spatio-temporal discretization for pedestrian flow characterization. Transport. Res. Part C (2017), http://dx.doi.org/10.1016/j.trc.2017.08.026

We can deal with sampled data in two ways. First, we generate trajectories using linear interpolation (Fig. 5). The speed along trajectories is approximated, using finite differences. The indicators are then obtained via 3DVoro applied to the interpolated trajectories. In the second case we apply 3DVoro directly to the sampled data. The indicators calculated on the true synthetic trajectories, generated using minimal step, are used as a benchmark. The indicators obtained using samples and interpolated trajectories are compared at 1000 randomly selected points to the corresponding benchmark values. These points are the same across all the methods.

We list in Tables 2 and 3 the statistics (mean, mode, median and 90%-quantile) corresponding to resulting differences in the case of density indicator, for $Uni_{LD-HomoPop}$, respectively $Uni_{HD-HeteroPop}$. The statistics show similar trends for velocity and flow indicators, as illustrated in Appendix A (Tables A.6–A.9). To demonstrate the performance, we show the results corresponding to the extreme values of the considered sampling frequencies (3 s^{-1} and 0.5 s^{-1}). In the tables, IT refers to the value of a given statistic obtained based on interpolated trajectories; SoP refers to the value of a given statistic obtained based on sample of points. Gray color of the cells in the tables is used to indicate the overall best value of the considered statistic. Note that in this case the E-3DVoro and the XY-T method can be applied only when the points from samples are interpolated.

Table 2
Robustness to the sampling frequency of density indicator – $Uni_{LD-HomoPop}$.

(a) Sampling frequency: 3 s^{-1};

Method	Mean		Mode		Median		90% quantile	
	IT	SoP	IT	SoP	IT	SoP	IT	SoP
XY-T	$1.47e^{-02}$	/	$1.25e^{-02}$	/	$1.25e^{-02}$	/	$6.25e^{-02}$	/
E-3DVoro	$1.17e^{-02}$	/	0	/	$4.48e^{-04}$	/	$3.96e^{-02}$	/
TT_1-3DVoro	$2.70e^{-03}$	$6.70e^{-03}$	0	0	$3.00e^{-04}$	$2.30e^{-03}$	$7.30e^{-03}$	$1.02e^{-02}$
TT_2-3DVoro	$5.80e^{-03}$	$3.50e^{-02}$	0	$2.80e^{-03}$	$6.00e^{-04}$	$2.08e^{-02}$	$1.50e^{-02}$	$6.69e^{-02}$
TT_3-3DVoro	$5.40e^{-03}$	$4.34e^{-02}$	0	$8.00e^{-03}$	$6.00e^{-04}$	$2.83e^{-02}$	$1.32e^{-02}$	$9.22e^{-02}$
P-3DVoro	$8.20e^{-03}$	$5.36e^{-02}$	0	$6.10e^{-03}$	$2.40e^{-03}$	$3.03e^{-02}$	$1.30e^{-02}$	$1.14e^{-01}$
M-3DVoro	$4.50e^{-03}$	$5.65e^{-02}$	0	$6.80e^{-03}$	$1.10e^{-03}$	$4.55e^{-02}$	$1.28e^{-02}$	$1.04e^{-01}$

(b) Sampling frequency: 0.5 s^{-1}.

Method	Mean		Mode		Median		90% quantile	
	IT	SoP	IT	SoP	IT	SoP	IT	SoP
XY-T	$1.90e^{-01}$	/	$1.00e^{-01}$	/	$1.50e^{-01}$	/	$3.38e^{-01}$	/
E-3DVoro	$1.64e^{-01}$	/	$1.12e^{-02}$	/	$1.46e^{-01}$	/	$3.02e^{-01}$	/
TT_1-3DVoro	$2.54e^{-01}$	$1.27e^{-01}$	$1.35e^{-02}$	$9.00e^{-03}$	$1.16e^{-01}$	$8.97e^{-02}$	$3.41e^{-01}$	$2.25e^{-01}$
TT_2-3DVoro	$1.64e^{-01}$	$1.22e^{-01}$	$1.44e^{-02}$	$1.06e^{-02}$	$1.21e^{-01}$	$7.30e^{-02}$	$3.52e^{-01}$	$2.33e^{-01}$
TT_3-3DVoro	$1.89e^{-01}$	$1.24e^{-01}$	$1.84e^{-02}$	$1.09e^{-02}$	$1.24e^{-01}$	$7.88e^{-02}$	$3.40e^{-01}$	$2.31e^{-01}$
P-3DVoro	$3.19e^{-01}$	$1.21e^{-01}$	$3.26e^{-02}$	$6.20e^{-03}$	$1.43e^{-01}$	$7.43e^{-02}$	$3.36e^{-01}$	$2.10e^{-01}$
M-3DVoro	$1.97e^{-01}$	$1.24e^{-01}$	$3.48e^{-02}$	$9.90e^{-03}$	$1.41e^{-01}$	$7.72e^{-02}$	$3.21e^{-01}$	$2.31e^{-01}$

Table 3
Robustness to the sampling frequency of density indicator – $Uni_{HD-HeteroPop}$.

(a) Sampling frequency: 3 s^{-1};

Method	Mean		Mode		Median		90% quantile	
	IT	SoP	IT	SoP	IT	SoP	IT	SoP
XY-T	$2.05e^{-02}$	/	0	/	$1.25e^{-02}$	/	$5.00e^{-02}$	/
E-3DVoro	$1.43e^{-02}$	/	0	/	$2.67e^{-02}$	/	$2.64e^{-02}$	/
TT_1-3DVoro	$8.00e^{-03}$	$4.55e^{-02}$	0	0	$8.00e^{-04}$	$1.75e^{-02}$	$2.36e^{-02}$	$8.52e^{-02}$
TT_2-3DVoro	$1.49e^{-02}$	$1.07e^{-01}$	0	0	$3.20e^{-03}$	$5.72e^{-02}$	$3.33e^{-02}$	$2.21e^{-01}$
TT_3-3DVoro	$1.24e^{-02}$	$1.60e^{-01}$	0	0	$3.50e^{-03}$	$9.62e^{-02}$	$2.98e^{-02}$	$3.41e^{-01}$
P-3DVoro	$2.10e^{-02}$	$1.66e^{-01}$	0	0	$4.20e^{-03}$	$1.16e^{-01}$	$5.27e^{-02}$	$3.64e^{-01}$
M-3DVoro	$1.31e^{-02}$	$2.40e^{-01}$	0	0	$2.50e^{-03}$	$1.75e^{-01}$	$2.91e^{-02}$	$5.58e^{-01}$

(b) Sampling frequency: 0.5 s^{-1}.

Method	Mean		Mode		Median		90% quantile	
	IT	SoP	IT	SoP	IT	SoP	IT	SoP
XY-T	$5.29e^{-01}$	/	$1.63e^{-01}$	/	$4.75e^{-01}$	/	$1.01e^{00}$	/
E-3DVoro	$4.02e^{-01}$	/	0	/	$2.49e^{-01}$	/	1.03E+00	/
TT_1-3DVoro	$4.06e^{-01}$	$2.90e^{-01}$	$3.10e^{-01}$	$2.48e^{-02}$	$2.64e^{-01}$	$1.65e^{-01}$	$9.21e^{-01}$	$7.12e^{-01}$
TT_2-3DVoro	$3.92e^{-01}$	$4.58e^{-01}$	$2.85e^{-01}$	$2.34e^{-01}$	$2.48e^{-01}$	$2.34e^{-01}$	$9.30e^{-01}$	1.11E+00
TT_3-3DVoro	$4.41e^{-01}$	$5.07e^{-01}$	$2.89e^{-01}$	$5.89e^{-02}$	$2.37e^{-01}$	$3.06e^{-01}$	$9.81e^{-01}$	1.17E+00
P-3DVoro	$4.31e^{-01}$	$3.71e^{-01}$	$1.40e^{-03}$	0	$2.58e^{-01}$	$1.80e^{-01}$	$9.43e^{-01}$	$7.29e^{-01}$
M-3DVoro	$4.34e^{-01}$	$5.01e^{-01}$	$3.16e^{-01}$	$1.36e^{-01}$	$2.75e^{-01}$	$3.52e^{-01}$	$9.96e^{-01}$	$9.80e^{-01}$

Please cite this article in press as: Nikolić, M., Bierlaire, M. Data-driven spatio-temporal discretization for pedestrian flow characterization. Transport. Res. Part C (2017), http://dx.doi.org/10.1016/j.trc.2017.08.026

In general, the 3DVoro method outperforms the XY-T method. The lowest differences between the indicators calculated based on sample of points or interpolated trajectories and the benchmark vales are achieved using the 3DVoro method.

The interpolation appears to be a better choice for 3DVoro when the sampling frequency is high, in both scenarios. This is expected, given that more data points used for interpolation yield lower interpolation error. In this case, the Time-Transform distances lead to the best performance of the 3DVoro approach, and in particular TT_1-3DVoro.

When the sampling frequency is low, 3DVoro applied directly to the sample is associated with the best effectiveness. In $Uni_{LD-HomoPop}$, the distances that take into account the speed and/or direction of pedestrians (in particular TT_2-3DVoro, P-3DVoro and M-3DVoro) are the most satisfactory. In $Uni_{HD-HeteroPop}$, the preferred characterization is based on the Time-Transform distances (particularly TT_1-3DVoro).

We have also analyzed the robustness to the sampling frequency for bi-directional flow composition and for both scenarios, $Bi_{LD-HomoPop}$ and $Bi_{HD-HeteroPop}$. Tables 4 and 5 report the statistics corresponding to resulting differences in the case of density indicator. The statistics show similar trends as for the uni-directional flow composition.

Table 4
Robustness to the sampling frequency of density indicator – $Bi_{LD-HomoPop}$.

(a) Sampling frequency: 3 s^{-1};

Method	Mean		Mode		Median		90% quantile	
	IT	SoP	IT	SoP	IT	SoP	IT	SoP
XY-T	$6.50e^{-02}$	/	0	/	0	/	$8.65e^{-03}$	/
E-3DVoro	$1.20e^{-02}$	/	0	/	0	/	$4.66e^{-03}$	/
TT_1-3DVoro	$3.58e^{-03}$	$1.08e^{-02}$	0	0	0	$1.02e^{-03}$	$4.16e^{-03}$	$6.15e^{-03}$
$TT_2$3DVoro	$8.13e^{-03}$	$1.18e^{-02}$	0	0	0	$2.35e^{-03}$	$8.09e^{-03}$	$1.29e^{-02}$
TT_3-3DVoro	$1.49e^{-02}$	$2.06e^{-02}$	0	$3.91e^{-03}$	0	$8.43e^{-03}$	$7.46e^{-03}$	$3.10e^{-02}$
P-3DVoro	$2.29e^{-02}$	$5.42e^{-02}$	0	$1.94e^{-03}$	0	$2.72e^{-02}$	$9.25e^{-03}$	$1.06e^{-01}$
M-3DVoro	$2.15e^{-02}$	$4.82e^{-02}$	0	$4.31e^{-02}$	0	$2.42e^{-02}$	$7.69e^{-03}$	$1.29e^{-01}$

(b) Sampling frequency: 0.5 s^{-1}.

Method	Mean		Mode		Median		90% quantile	
	IT	SoP	IT	SoP	IT	SoP	IT	SoP
XY-T	$1.66e^{-01}$	/	0	/	$6.84e^{-02}$	/	$7.00e^{-01}$	/
E-3DVoro	$1.65e^{-01}$	/	0	/	$1.19e^{-01}$	/	$3.40e^{-01}$	/
TT_1-3DVoro	$1.68e^{-01}$	$1.29e^{-01}$	$3.50e^{-02}$	$5.02e^{-02}$	$8.50e^{-02}$	$5.70e^{-02}$	$3.85e^{-01}$	$2.62e^{-01}$
TT_2-3DVoro	$1.70e^{-01}$	$1.02e^{-01}$	$4.52e^{-02}$	$5.63e^{-02}$	$8.49e^{-02}$	$6.15e^{-02}$	$3.82e^{-01}$	$5.57e^{-01}$
TT_3-3DVoro	$1.80e^{-01}$	$1.18e^{-01}$	$4.82e^{-02}$	$6.06e^{-02}$	$8.80e^{-02}$	$6.55e^{-02}$	$3.83e^{-01}$	$2.65e^{-01}$
P-3DVoro	$2.02e^{-01}$	$1.60e^{-01}$	$3.69e^{-02}$	$4.84e^{-02}$	$9.36e^{-02}$	$6.73e^{-02}$	$4.14e^{-01}$	$3.01e^{-01}$
M-3DVoro	$1.80e^{-01}$	$1.55e^{-01}$	$4.80e^{-02}$	$3.36e^{-02}$	$1.01e^{-01}$	$9.27e^{-02}$	$4.38e^{-01}$	$3.08e^{-01}$

Table 5
Robustness to the sampling frequency of density indicator – $Bi_{HD-HeteroPop}$.

(a) Sampling frequency: 3 s^{-1};

Method	Mean		Mode		Median		90% quantile	
	IT	SoP	IT	SoP	IT	SoP	IT	SoP
XY-T	$2.85e^{-02}$	/	0	/	$3.28e^{-03}$	/	$1.00e^{-01}$	/
E-3DVoro	$3.00e^{-02}$	/	0	/	$9.64e^{-03}$	/	$6.50e^{-02}$	/
TT_1-3DVoro	$1.15e^{-01}$	$2.78e^{-02}$	0	0	$7.90e^{-04}$	$8.78e^{-03}$	$2.32e^{-02}$	$4.94e^{-02}$
TT_2-3DVoro	$9.72e^{-02}$	$9.34e^{-02}$	0	0	$3.21e^{-03}$	$5.16e^{-02}$	$3.50e^{-02}$	$2.15e^{-01}$
TT_3-3DVoro	$4.89e^{-02}$	$1.05e^{-01}$	0	0	$2.83e^{-03}$	$5.91e^{-02}$	$3.56e^{-02}$	$2.62e^{-01}$
P-3DVoro	$1.15e^{-01}$	$1.70e^{-01}$	0	$3.33e^{-02}$	$4.79e^{-03}$	$6.28e^{-02}$	$4.65e^{-02}$	$2.61e^{-01}$
M-3DVoro	$1.15e^{-01}$	$1.52e^{-01}$	0	$8.33e^{-02}$	$4.55e^{-03}$	$7.20e^{-02}$	$5.35e^{-02}$	$3.51e^{-01}$

(b) Sampling frequency: 0.5 s^{-1}.

Method	Mean		Mode		Median		90% quantile	
	IT	SoP	IT	SoP	IT	SoP	IT	SoP
XY-T								
E-3DVoro	$2.79e^{-01}$	/	0	/	$1.29e^{-01}$	/	$7.14e^{-01}$	/
TT_1-3DVoro	$4.49e^{-01}$	$2.58e^{-01}$	$5.70e^{-03}$	$1.99e^{-03}$	$1.54e^{-01}$	$1.34e^{-01}$	$8.43e^{-01}$	$6.64e^{-01}$
TT_2-3DVoro	$3.71e^{-01}$	$2.98e^{-01}$	$4.28e^{-02}$	$9.34e^{-02}$	$1.61e^{-01}$	$1.40e^{-01}$	$8.07e^{-01}$	$7.90e^{-01}$
TT_3-3DVoro	$9.82e^{-01}$	$3.56e^{-01}$	$4.34e^{-02}$	$6.70e^{-03}$	$1.64e^{-01}$	$1.38e^{-01}$	$7.76e^{-01}$	$7.74e^{-01}$
P-3DVoro	$3.82e^{-01}$	$3.15e^{-01}$	$2.32e^{-03}$	$6.74e^{-03}$	$1.53e^{-01}$	$1.61e^{-01}$	$9.09e^{-01}$	$7.22e^{-01}$
M-3DVoro	$4.08e^{-01}$	$3.77e^{-01}$	$1.89e^{-02}$	$1.47e^{-02}$	$1.90e^{-01}$	$1.74e^{-01}$	$7.91e^{-01}$	$8.18e^{-01}$

Please cite this article in press as: Nikolić, M., Bierlaire, M. Data-driven spatio-temporal discretization for pedestrian flow characterization. Transport. Res. Part C (2017), http://dx.doi.org/10.1016/j.trc.2017.08.026

In summary, the *Time-Transform 3D Voronoi characterization* is the most robust with respect to the sampling frequency when more data is available (the sampling frequency equal to 3 s^{-1} or the demand equal to 3.6 pedestrians per second). When less data is available (the sampling frequency equal to 0.5 s^{-1} and the demand equal to 1.2 pedestrians per second), the distances accounting for the dynamics of pedestrians lead to the best robustness with respect to the sampling.

6. Conclusion

In this paper a novel methodology for pedestrian traffic characterization is proposed. The definitions of pedestrian traffic variables that we have put forward are based on data-driven partitioning in space and time, avoiding the need to define an arbitrary discretization. The disretization framework is designed via three-dimensional Voronoi diagrams directly generated from pedestrian trajectory data. It can be designed based on trajectories available either in the form of an analytical description or as a finite collection of points. The methodological framework is fairly general, and the exact characterization of the Voronoi diagrams can be adapted to specific situations. We have proposed different definitions of distances for the construction of the diagrams, and assessed them in quantitative terms. Also, the proposed definitions of the indicators are microscopic. They are therefore able to reflect the heterogeneity of pedestrians, and suitable for the multi-directional composition of pedestrian flows.

The performance of the proposed approach is evaluated using synthetic data. It has been shown, for these data sets, that our approach outperforms the considered approaches from the literature, in terms of the robustness to the simulation noise and the robustness with respect to the sampling frequency. As for the robustness to the simulation noise, 3DVoro with distances that account for the speed and/or movement direction of pedestrians lead to lower variance in the results when demand is low. When demand is higher, higher number of data leads to similar behavior of different distances. As for the robustness to the sampling frequency, when the sampling frequency is high, 3DVoro based on interpolated trajectories shows better results. When the sampling frequency is low, 3DVoro based on sample of points exhibit better performance. The analysis in the case of sampled data suggests that (i) when more data is available, either because of higher sampling frequency (3 s^{-1}) or higher demand (3.6 pedestrians per second), TT_1-3DVoro is the most robust with respect to the sampling frequency; (ii) when less data is available, due to lower sampling frequency (0.5 s^{-1}) and lighter traffic conditions (the demand of 1.2 pedestrians per second), the distances that account for the speed and the movement direction of pedestrians (TT_2-3DVoro, P-3DVoro and M-3DVoro) exhibit the best robustness.

Detailed observations on pedestrian movements allow for new empirical findings. These findings consequently support the development of solid, empirically supported theoretical and conceptual basis, and finally the development of powerful models. This is achievable only if the methods used for the measurement and analysis are in compliance with the nature and the resolution of the data. Otherwise, the potential of the data is reduced or completely eliminated. Our approach to pedestrian flow characterization utilizes the gain obtained using new data collection technologies. Being entirely adjusted to the data, it allows for the revelation of new empirical phenomena. This has a direct effect on pedestrian flow modeling, by influencing the modeling approach and underlying assumptions (Nikolić et al., 2016).

More research is needed to determine the performance of the approach in other behavioral situations and to understand its potential limitations. In our future research, we will examine the effectiveness of the approach using real data (described in Nikolić et al. (2016)). A sensitivity analysis for the conversion parameter v in TT_1-3DVoro, and the α parameter in M-3DVoro is another direction of the investigation.

The set of distances proposed in this paper to characterize the Voronoi diagrams can be extended. In particular, an interesting research topic would be to relate the definition of the distance with some behavioral assumptions about the pedestrian movements. For example, it has been recognized that pedestrians are affected much stronger by stimuli that appear within their vision field (Johansson et al., 2007). To account for the anisotropy of pedestrian movements, weighted versions of the proposed distances could be further studied. The weights would be modeled based on the movement direction of pedestrians and their vision field.

Our future research will also be directed towards the characterization in the presence of obstacles. One possibility would be to extend a generator set from pedestrian trajectories to trajectories and areas, where areas represent obstacles. This would result in three-dimensional discretization where each pedestrian and each obstacle are associated with their own, non-overlaping, spatio-temporal units.

Acknowledgements

This research is supported by the Swiss National Science Foundation Grant 200021-141099 "Pedestrian dynamics: flows and behavior". We would like to thank Flurin Hänseler, Shadi Sharif Azadeh and Riccardo Scarinci for their invaluable assistance and suggestions. We are thankful for the constructive comments obtained from the audience in several research conferences (Swiss Transport Research Conference, International Conference on Pedestrian and Evacuation Dynamics, Conference on Traffic and Granular Flow, European Association of Research in Transportation, Triennial Symposium on Transportation Analysis), where different development phases of our methodological framework were presented.

Please cite this article in press as: Nikolić, M., Bierlaire, M. Data-driven spatio-temporal discretization for pedestrian flow characterization. Transport. Res. Part C (2017), http://dx.doi.org/10.1016/j.trc.2017.08.026

Appendix A. Robustness to the sampling frequency of velocity and flow indicators

It is interesting to notice that the XY-T method results in the most satisfactory estimation of speed only in $S_{LC-HomoPop}$ for high sampling frequency (Table A.6(a)). This can be explained by the simulated homogenous speed conditions that the fixed-grid discretization is able to reflect. When the sampling frequency is lower (Table A.6(b)), or when traffic conditions are more complex (Table A.7), the performance of this method deteriorates, in regard to the speed estimation.

Table A.6
Robustness to the sampling frequency of velocity indicator – $Uni_{LD-HomoPop}$.

(a) Sampling frequency: 3 s^{-1};

Method	Mean		Mode		Median		90% quantile	
	IT	SoP	IT	SoP	IT	SoP	IT	SoP
XY-T	$4.30e^{-03}$	/	0	/	$3.40e^{-03}$	/	$1.16e^{-02}$	/
E-3DVoro	$1.55e^{-01}$	/	0	/	$3.56e^{-02}$	/	$4.99e^{-01}$	/
TT_1-3DVoro	$9.60e^{-03}$	$2.31e^{-02}$	0	0	$2.20e^{-03}$	$9.38e^{-03}$	$2.79e^{-02}$	$4.85e^{-02}$
TT_2-3DVoro	$2.04e^{-02}$	$7.66e^{-02}$	0	$4.10e^{-03}$	$5.80e^{-03}$	$4.48e^{-02}$	$6.48e^{-02}$	$1.68e^{-01}$
TT_3-3DVoro	$1.81e^{-02}$	$9.15e^{-02}$	0	$8.00e^{-04}$	$5.70e^{-03}$	$4.51e^{-02}$	$5.42e^{-02}$	$2.15e^{-01}$
P-3DVoro	$2.98e^{-02}$	$1.38e^{-01}$	0	$5.90e^{-03}$	$1.41e^{-02}$	$7.90e^{-02}$	$5.75e^{-02}$	$2.92e^{-01}$
M-3DVoro	$1.88e^{-02}$	$1.46e^{-01}$	0	$2.00e^{-04}$	$5.90e^{-03}$	$1.04e^{-01}$	$5.95e^{-02}$	$3.22e^{-01}$

(b) Sampling frequency: 0.5 s^{-1}.

Method	Mean		Mode		Median		90% quantile	
	IT	SoP	IT	SoP	IT	SoP	IT	SoP
XY-T	$5.80e^{-01}$	/	$1.02e^{00}$	/	$3.26e^{-01}$	/	$1.42e^{00}$	/
E-3DVoro	$1.77e^{00}$	/	$4.36e^{-02}$	/	$7.11e^{-01}$	/	$1.27e^{00}$	/
TT_1-3DVoro	$5.42e^{-01}$	$5.40e^{-01}$	$2.28e^{-02}$	$2.10e^{-03}$	$3.43e^{-01}$	$3.02e^{-01}$	$1.04e^{00}$	$9.66e^{-01}$
TT_2-3DVoro	$5.11e^{-01}$	$5.56e^{-01}$	$1.39e^{-01}$	$8.20e^{-03}$	$3.15e^{-01}$	$3.17e^{-01}$	$1.07e^{00}$	$1.04e^{00}$
TT_3-3DVoro	$6.08e^{-01}$	$5.52e^{-01}$	$3.72e^{-02}$	$7.50e^{-03}$	$3.29e^{-01}$	$3.18e^{-01}$	$1.05e^{00}$	$1.05e^{00}$
P-3DVoro	$5.60e^{-01}$	$5.41e^{-01}$	$8.75e^{-02}$	$1.30e^{-03}$	$3.32e^{-01}$	$3.04e^{-01}$	$9.76e^{-01}$	$9.82e^{-01}$
M-3DVoro	$5.03e^{-01}$	$5.43e^{-01}$	$3.93e^{-02}$	$6.91e^{-02}$	$3.76e^{-01}$	$3.15e^{-01}$	$1.08e^{00}$	$9.52e^{-01}$

Table A.7
Robustness to the sampling frequency of velocity indicator – $Uni_{HD-HeteroPop}$.

(a) Sampling frequency: 3 s^{-1};

Method	Mean		Mode		Median		90% quantile	
	IT	SoP	IT	SoP	IT	SoP	IT	SoP
XY-T	$1.92e^{-02}$	/	$9.60e^{-03}$	/	$6.20e^{-03}$	/	$3.42e^{-02}$	/
E-3DVoro	$3.17e^{-02}$	/	0	/	$6.30e^{-03}$	/	$3.86e^{-02}$	/
TT_1-3DVoro	$1.57e^{-02}$	$6.18e^{-02}$	0	0	$6.10e^{-03}$	$1.87e^{-02}$	$3.23e^{-02}$	$1.30e^{-01}$
TT_2-3DVoro	$1.83e^{-02}$	$1.38e^{-01}$	0	$1.73e^{-02}$	$7.90e^{-03}$	$4.27e^{-02}$	$3.82e^{-02}$	$3.88e^{-01}$
TT_3-3DVoro	$1.85e^{-02}$	$1.88e^{-01}$	0	$1.00e^{-01}$	$8.00e^{-03}$	$6.46e^{-02}$	$4.08e^{-02}$	$4.87e^{-01}$
P-3DVoro	$2.93e^{-02}$	$2.05e^{-01}$	0	$7.96e^{-02}$	$9.00e^{-03}$	$9.82e^{-02}$	$6.49e^{-02}$	$5.29e^{-01}$
M-3DVoro	$2.14e^{-02}$	$3.16e^{-01}$	0	$5.10e^{-03}$	$8.00e^{-03}$	$1.47e^{-01}$	$4.37e^{-02}$	$8.21e^{-01}$

(b) Sampling frequency: 0.5 s^{-1}.

Method	Mean		Mode		Median		90% quantile	
	IT	SoP	IT	SoP	IT	SoP	IT	SoP
XY-T	$5.73e^{-01}$	/	$1.15e^{00}$	/	$3.51e^{-01}$	/	$1.58e^{00}$	/
E-3DVoro	$1.01e^{00}$	/	$8.57e^{-01}$	/	$3.85e^{-01}$	/	$1.67e^{00}$	/
TT_1-3DVoro	$5.82e^{-01}$	$5.80e^{-01}$	$8.69e^{-01}$	$5.85e^{-02}$	$4.51e^{-01}$	$3.13e^{-01}$	$1.40e^{00}$	$1.28e^{00}$
TT_2-3DVoro	$5.76e^{-01}$	$5.67e^{-01}$	$9.40e^{-01}$	$1.02e^{-01}$	$3.75e^{-01}$	$2.64e^{-01}$	$1.54e^{00}$	$1.16e^{00}$
TT_3-3DVoro	$5.79e^{-01}$	$5.94e^{-01}$	$8.50e^{-01}$	$5.73e^{-02}$	$3.70e^{-01}$	$2.77e^{-01}$	$1.46e^{00}$	$1.29e^{00}$
P-3DVoro	$5.66e^{-01}$	$5.62e^{-01}$	$8.92e^{-01}$	$4.61e^{-02}$	$3.83e^{-01}$	$2.95e^{-01}$	$1.38e^{00}$	$1.26e^{00}$
M-3DVoro	$6.27e^{-01}$	$7.11e^{-01}$	$9.13e^{-01}$	$1.43e^{-02}$	$5.05e^{-01}$	$2.86e^{-01}$	$1.55e^{00}$	$1.49e^{00}$

Please cite this article in press as: Nikolić, M., Bierlaire, M. Data-driven spatio-temporal discretization for pedestrian flow characterization. Transport. Res. Part C (2017), http://dx.doi.org/10.1016/j.trc.2017.08.026

Table A.8
Robustness to the sampling frequency of flow indicator – $Uni_{LD-HomoPop}$.

(a) Sampling frequency: 3 s^{-1};

Method	Mean		Mode		Median		90% quantile	
	IT	SoP	IT	SoP	IT	SoP	IT	SoP
XY-T	$1.93e^{-02}$	/	0	/	$1.77e^{-02}$	/	$7.73e^{-02}$	/
E-3DVoro	$1.65e^{-02}$	/	0	/	$5.60e^{-03}$	/	$3.75e^{-02}$	/
TT_1-3DVoro	$3.00e^{-04}$	$7.60e^{-03}$	0	0	0	$2.60e^{-03}$	$8.00e^{-04}$	$1.74e^{-02}$
TT_2-3DVoro	$1.40e^{-03}$	$4.16e^{-02}$	0	0	0	$3.17e^{-02}$	$3.60e^{-03}$	$8.99e^{-02}$
TT_3-3DVoro	$1.30e^{-03}$	$4.65e^{-02}$	0	$4.32e^{-02}$	0	$3.48e^{-02}$	$3.90e^{-03}$	$1.14e^{-01}$
P-3DVoro	$2.70e^{-03}$	$4.69e^{-02}$	0	$1.41e^{-02}$	$8.00e^{-04}$	$2.27e^{-02}$	$5.50e^{-03}$	$1.29e^{-01}$
M-3DVoro	$1.20e^{-03}$	$5.09e^{-02}$	0	$4.75e^{-02}$	0	$3.54e^{-02}$	$2.50e^{-03}$	$1.23e^{-01}$

(b) Sampling frequency: 0.5 s^{-1}.

Method	Mean		Mode		Median		90% quantile	
	IT	SoP	IT	SoP	IT	SoP	IT	SoP
XY-T	$2.55e^{-01}$	/	$1.45e^{-01}$	/	$2.45e^{-01}$	/	$5.06e^{-01}$	/
E-3DVoro	$4.17e^{-01}$	/	$6.50e^{-02}$	/	$1.27e^{-01}$	/	$3.83e^{-01}$	/
3DVoro-δ_{TT_1}	$1.74e^{-01}$	$1.50e^{-01}$	$1.79e^{-01}$	$8.00e^{-04}$	$1.13e^{-01}$	$8.77e^{-02}$	$3.21e^{-01}$	$2.98e^{-01}$
TT_1-3DVoro	$2.07e^{-01}$	$1.53e^{-01}$	$1.92e^{-01}$	$1.00e^{-04}$	$1.39e^{-01}$	$8.52e^{-02}$	$3.71e^{-01}$	$3.29e^{-01}$
TT_2-3DVoro	$2.33e^{-01}$	$1.52e^{-01}$	$2.05e^{-01}$	$3.00e^{-04}$	$1.48e^{-01}$	$8.46e^{-02}$	$3.63e^{-01}$	$3.27e^{-01}$
TT_2-3DVoro	$2.17e^{-01}$	$1.43e^{-01}$	$1.53e^{-01}$	$1.40e^{-03}$	$1.34e^{-01}$	$8.49e^{-02}$	$3.01e^{-01}$	$2.98e^{-01}$
M-3DVoro	$1.75e^{-01}$	$1.48e^{-01}$	$1.83e^{-01}$	$1.00e^{-04}$	$1.36e^{-01}$	$9.11e^{-02}$	$3.43e^{-01}$	$3.22e^{-01}$

Table A.9
Robustness to the sampling frequency of flow indicator – $Uni_{HD-HeteroPop}$.

(a) Sampling frequency: 3 s^{-1};

Method	Mean		Mode		Median		90% quantile	
	IT	SoP	IT	SoP	IT	SoP	IT	SoP
XY-T	$2.75e^{-02}$	/	$2.30e^{-03}$	/	$1.75e^{-02}$	/	$7.21e^{-02}$	/
E-3DVoro	$1.09e^{-02}$	/	0	/	$8.70e^{-04}$	/	$2.83e^{-02}$	/
TT_1-3DVoro	$7.80e^{-03}$	$6.06e^{-02}$	0	0	$7.00e^{-04}$	$1.21e^{-02}$	$2.22e^{-02}$	$1.58e^{-01}$
TT_2-3DVoro	$1.05e^{-02}$	$1.45e^{-01}$	0	0	$1.10e^{-03}$	$6.08e^{-02}$	$2.78e^{-02}$	$3.11e^{-01}$
TT_3-3DVoro	$1.06e^{-02}$	$2.03e^{-01}$	0	0	$1.00e^{-03}$	$8.27e^{-02}$	$2.19e^{-02}$	$4.64e^{-01}$
P-3DVoro	$1.62e^{-02}$	$1.95e^{-01}$	0	$4.86e^{-02}$	$1.80e^{-03}$	$8.54e^{-02}$	$3.70e^{-02}$	$4.90e^{-01}$
M-3DVoro	$1.29e^{-02}$	$3.06e^{-01}$	0	0	$1.60e^{-03}$	$1.48e^{-01}$	$2.92e^{-02}$	$8.95e^{-01}$

(b) Sampling frequency: 0.5 s^{-1}.

Method	Mean		Mode		Median		90% quantile	
	IT	SoP	IT	SoP	IT	SoP	IT	SoP
XY-T	$5.18e^{-01}$	/	$3.50e^{-01}$	/	$4.48e^{-01}$	/	$1.09e^{00}$	/
E-3DVoro	$6.54e^{-01}$	/	$3.69e^{-01}$	/	$2.03e^{-01}$	/	$1.54e^{00}$	/
TT_1-3DVoro	$4.99e^{-01}$	$4.02e^{-01}$	$1.06e^{-01}$	$6.49e^{-02}$	$3.24e^{-01}$	$1.81e^{-01}$	$1.35e^{00}$	$9.43e^{-01}$
TT_2-3DVoro	$5.66e^{-01}$	$4.16e^{-01}$	$1.47e^{-01}$	$5.55e^{-02}$	$2.73e^{-01}$	$1.73e^{-01}$	$1.57e^{00}$	$1.21e^{00}$
TT_3-3DVoro	$5.91e^{-01}$	$4.45e^{-01}$	$1.53e^{-01}$	$1.57e^{-01}$	$2.94e^{-01}$	$1.71e^{-01}$	$1.68e^{00}$	$1.31e^{00}$
P-3DVoro	$4.81e^{-01}$	$4.28e^{-01}$	$5.53e^{-02}$	$3.98e^{-02}$	$2.22e^{-01}$	$1.89e^{-01}$	$1.34e^{00}$	$1.12e^{00}$
M-3DVoro	$6.41e^{-01}$	$4.47e^{-01}$	$9.07e^{-02}$	$4.55e^{-02}$	$3.97e^{-01}$	$1.73e^{-01}$	$1.66e^{00}$	$1.24e^{00}$

References

Alahi, A., Bierlaire, M., Vandergheynst, P., 2014a. Robust real-time pedestrians detection in urban environments with a network of low resolution cameras. Transport. Res. Part C: Emerg. Technol. 39, 113–128.

Alahi, A., Bierlaire, M., Vandergheynst, P., 2014b. Robust real-time pedestrians detection in urban environments with low-resolution cameras. Transport. Res. Part C: Emerg. Technol. 39, 113–128.

Alahi, A., Jacques, L., Boursier, Y., Vandergheynst, P., 2011. Sparsity driven people localization with a heterogeneous network of cameras. J. Math. Imag. Vis. 41 (1–2), 39–58.

Bauer, D., Brandle, N., Seer, S., Ray, M., Kitazawa, K., 2009. Measurement of pedestrian movements: a comparative study on various existing systems. In: Pedestrian Behavior: Models, Data Collection and Applications. Emerald Group Publishing Limited, Bingley, UK.

Beck, C., Roepstorff, G., 1987. Effects of phase space discretization on the long-time behavior of dynamical systems. Phys. D: Nonlin. Phenom. 25 (1–3), 173–180.

Please cite this article in press as: Nikolić, M., Bierlaire, M. Data-driven spatio-temporal discretization for pedestrian flow characterization. Transport. Res. Part C (2017), http://dx.doi.org/10.1016/j.trc.2017.08.026

Bierlaire, M., Robin, T., 2009. Pedestrians choices. Pedestrian Behav., 1–26
Blue, V.J., Adler, J.L., 2001. Cellular automata microsimulation for modeling bi-directional pedestrian walkways. Transport. Res. Part B: Methodol. 35 (3), 293–312.
Bovy, P.H., Stern, E., 2012. Route Choice: Wayfinding in Transport Networks: Wayfinding in Transport Networks, vol. 9. Springer Science & Business Media.
Campanella, M., Hoogendoorn, S., Daamen, W., 2014. The nomad model: theory, developments and applications. Transport. Res. Proc. 2, 462–467.
Cheah, J.Y., Smith, J.M., 1994. Generalized M/G/c/c state dependent queueing models and pedestrian traffic flows. Queueing Syst. 15 (1–4), 365–386.
Cheung, C., Lam, W.H., 1998. Pedestrian route choices between escalator and stairway in MTR stations. J. Transport. Eng. 124 (3), 277–285.
Çöltekin, A., De Sabbata, S., Willi, C., Vontobel, I., Pfister, S., Kuhn, M., Lacayo, M., 2011. Modifiable temporal unit problem. In: ISPRS/ICA Workshop Persistent Problems in Geographic Visualization (ICC2011), Paris, France, vol. 2.
Daamen, W., 2004. Modelling Passenger Flows in Public Transport Facilities. Ph.D. thesis, Delft University of Technology, Delft.
Daamen, W., Hoogendoorn, S.P., 2003. Controlled experiments to derive walking behaviour. Eur. J. Transp. Infrastruct. Res. 3 (1), 39–59.
Danalet, A., Farooq, B., Bierlaire, M., 2014. A bayesian approach to detect pedestrian destination-sequences from WiFi signatures. Transport. Res. Part C: Emerg. Technol. 44, 146–170.
Duives, D., 2012. Analysis of Pedestrian Crowd Movements at Lowlands. Ph.D. thesis, TU Delft, Delft University of Technology.
Duives, D.C., Daamen, W., Hoogendoorn, S.P., 2013. State-of-the-art crowd motion simulation models. Transport. Res. Part C: Emerg. Technol. 37, 193–209.
Duives, D.C., Daamen, W., Hoogendoorn, S.P., 2015. Quantification of the level of crowdedness for pedestrian movements. Phys. A: Stat. Mech. Appl. 427, 162–180.
Edie, L.C., 1963. Discussion of Traffic Stream Measurements and Definitions. Port of New York Authority.
Fruin, J.J., 1971. Designing for Pedestrians: A Level-of-service Concept. No. 355. Highway Research Board, Washington, DC, pp. 1–15.
Fuchida, T., Kashima, M., Nakamura, H., Mori, K., Murashima, S., 2005. Constructing three-dimensional discrete Voronoi diagrams by the incremental method and application to self-organizing maps. Syst. Comput. Jpn. 36 (5), 55–67.
Helbing, D., Buzna, L., Johansson, A., Werner, T., 2005. Self-organized pedestrian crowd dynamics: experiments, simulations, and design solutions. Transport. Sci. 39 (1), 1–24.
Helbing, D., Johansson, A., 2010. Pedestrian, crowd and evacuation dynamics. Encyclopedia Complex. Syst. Sci. 16, 6476–6495.
Helbing, D., Johansson, A., Al-Abideen, H.Z., 2007. Dynamics of crowd disasters: an empirical study. Phys. Rev. E 75 (4), 046109.
Helbing, D., Molnar, P., 1995. Social force model for pedestrian dynamics. Phys. Rev. E 51 (5), 4282–4286.
Hoff III, K.E., Keyser, J., Lin, M., Manocha, D., Culver, T., 1999. Fast computation of generalized Voronoi diagrams using graphics hardware. In: Proceedings of the 26th annual conference on Computer graphics and interactive techniques. ACM Press/Addison-Wesley Publishing Co, pp. 277–286.
Hoogendoorn, S., Daamen, W., 2004. Self-organization in walker experiments. In: Traffic and Granular Flow, vol. 3. pp. 121–132.
Hoogendoorn, S., HL Bovy, P., 2003. Simulation of pedestrian flows by optimal control and differential games. Optim. Contr. Appl. Methods 24 (3), 153–172.
Hoogendoorn, S.P., Bovy, P.H., 2004. Pedestrian route-choice and activity scheduling theory and models. Transport. Res. Part B: Methodol. 38 (2), 169–190.
Hoogendoorn, S.P., Daamen, W., 2005. Pedestrian behavior at bottlenecks. Transport. Sci. 39 (2), 147–159.
Hoogendoorn, S.P., van Wageningen-Kessels, F., Daamen, W., Duives, D.C., Sarvi, M., 2015. Continuum theory for pedestrian traffic flow: local route choice modelling and its implications. Transport. Res. Part C: Emerg. Technol. 59, 183–197.
Hoogendoorn, S.P., van Wageningen-Kessels, F.L., Daamen, W., Duives, D.C., 2014. Continuum modelling of pedestrian flows: from microscopic principles to self-organised macroscopic phenomena. Phys. A: Stat. Mech. Appl. 416, 684–694.
Hsu, J.-J., Chu, J.C., 2014. Long-term congestion anticipation and aversion in pedestrian simulation using floor field cellular automata. Transport. Res. Part C: Emerg. Technol. 48, 195–211.
Hughes, R.L., 2002. A continuum theory for the flow of pedestrians. Transport. Res. Part B: Methodol. 36 (6), 507–535.
Jabari, S.E., Zheng, J., Liu, H.X., 2014. A probabilistic stationary speed–density relation based on Newell's simplified car-following model. Transport. Res. Part B: Methodol. 68, 205–223.
Johansson, A., Helbing, D., Shukla, P.K., 2007. Specification of the social force pedestrian model by evolutionary adjustment to video tracking data. Adv. Complex Syst. 10 (supp02), 271–288.
Lam, W.H., Morrall, J.F., Ho, H., 1995. Pedestrian flow characteristics in Hong Kong. Transport. Res. Rec. (1487), 56–62
Løvås, G.G., 1994. Modeling and simulation of pedestrian traffic flow. Transport. Res. Part B: Methodol. 28 (6), 429–443.
Nikolić, M., Bierlaire, M., 2014. Pedestrian-oriented flow characterization. Transport. Res. Proc. 2, 359–366.
Nikolić, M., Bierlaire, M., 2015. Pedestrian flow characterization based on spatio-temporal voronoi tessellations. In: 15th Swiss Transportation Research Conference, No. 679, pp. 2101–2107.
Nikolić, M., Bierlaire, M., Farooq, B., de Lapparent, M., 2016. Probabilistic speed–density relationship for pedestrian traffic. Transport. Res. Part B: Methodol. 89, 58–81.
Okabe, A., Boots, B., Sugihara, K., Chiu, S.N., 2000. Spatial Tessellations: Concepts and Applications of Voronoi Diagrams. Wiley, New York.
Openshaw, S., 1984. The Modifiable Areal Unit Problem. Geo Abstracts University of East Anglia.
Park, S.W., Linsen, L., Kreylos, O., Owens, J.D., Hamann, B., 2006. Discrete Sibson interpolation. IEEE Trans. Vis. Comput. Graph. 12 (2), 243–253.
Rigaux, P., Scholl, M., Voisard, A., 2001. Spatial Databases: With Application to GIS. Morgan Kaufmann.
Robin, T., Antonini, G., Bierlaire, M., Cruz, J., 2009. Specification, estimation and validation of a pedestrian walking behavior model. Transport. Res. Part B: Methodol. 43 (1), 36–56.
Rong, G., Tan, T.-S., 2007. Variants of jump flooding algorithm for computing discrete Voronoi diagrams. In: 4th International Symposium on Voronoi Diagrams in Science and Engineering, 2007, ISVD'07. IEEE, pp. 176–181.
Saberi, M., Mahmassani, H.S., Director, T.C., 2014. Exploring area-wide dynamics of pedestrian crowds using a three-dimensional approach. In: Transportation Research Board 93rd Annual Meeting, No. 14-1609.
Schadschneider, A., Klingsch, W., Klüpfel, H., Kretz, T., Rogsch, C., Seyfried, A., 2009. Evacuation dynamics: empirical results, modeling and applications. In: Encyclopedia of Complexity and Systems Science. Springer.
Schueller, A., 2007. A nearest neighbor sweep circle algorithm for computing discrete Voronoi tessellations. J. Math. Anal. Appl. 336 (2), 1018–1025.
Seer, S., Brändle, N., Ratti, C., 2014. Kinects and human kinetics: a new approach for studying pedestrian behavior. Transport. Res. Part C: Emerg. Technol. 48, 212–228.
Steffen, B., Seyfried, A., 2010. Methods for measuring pedestrian density, flow, speed and direction with minimal scatter. Phys. A: Stat. Mech. Appl. 389 (9), 1902–1910.
Stubenschrott, M., Kogler, C., Matyus, T., Seer, S., 2014. A dynamic pedestrian route choice model validated in a high density subway station. Transport. Res. Proc. 2, 376–384.
Treiber, M., Kesting, A., 2013. Traffic flow dynamics. In: Traffic Flow Dynamics: Data, Models and Simulation. Springer-Verlag, Berlin Heidelberg.
Van der Putte, T., 2009. Using the Discrete 3d Voronoi Diagram for the Modelling of 3d Continuous Information in Geosciences. Ph.D. thesis, TU Delft, Delft University of Technology.
van Wageningen-Kessels, F., Hoogendoorn, S.P., Daamen, W., 2014. Extension of Edie's definitions for pedestrian dynamics. Transport. Res. Proc. 2, 507–512.
Weidmann, U., 1993. Transporttechnik der fussgänger. Tech. Rep. Schriftenreihe des IVT Nr. 90, Institut für Verkehrsplanung,Transporttechnik,Strassen- und Eisenbahnbau, ETH Zürich, (In German).
Zeng, W., Chen, P., Nakamura, H., Iryo-Asano, M., 2014. Application of social force model to pedestrian behavior analysis at signalized crosswalk. Transport. Res. Part C: Emerg. Technol. 40, 143–159.
Zhang, J., 2012. Pedestrian Fundamental Diagrams: Comparative Analysis of Experiments in Different Geometries. Ph.D. thesis, Forschungszentrum Jülich.

Please cite this article in press as: Nikolić, M., Bierlaire, M. Data-driven spatio-temporal discretization for pedestrian flow characterization. Transport. Res. Part C (2017), http://dx.doi.org/10.1016/j.trc.2017.08.026